The International Journal of Advanced Manufacturing Technology (2020) 108:1049–1059
https://doi.org/10.1007/s00170-019-04782-z

ORIGINAL ARTICLE

Effect of process parameters on mechanical properties of VeroBlue material and their optimal selection in PolyJet technology

Arivazhagan Pugalendhi[1] · Rajesh Ranganathan[1] · Manivannan Chandrasekaran[1]

Received: 12 June 2019 / Accepted: 3 December 2019 / Published online: 17 December 2019

Abstract
PolyJet technology is one of the additive manufacturing technologies, which can produce complex geometries with variety of textures. The 3D printed complex geometry parts need better mechanical behaviour. The mechanical properties of a fabricated product depend on several process parameters such as build orientation, layer thickness, material and surface finish. This paper aims to study the effect of printing mode and type of surface finish on the mechanical properties of VeroBlue material used in PolyJet technology. The tensile, flexural and shore hardness tests are carried out to determine the mechanical response of the fabricated specimen. Four different combinations are derived from printing mode (high quality (HQ) and high speed (HS)) and finish type (matte (M) and glossy (G)). Findings indicate the HS-G specimens have better mechanical property and are faster in production and cheaper than HQ-M, HQ-G and HS-M. Highest average tensile strength of the HS-G (49.77 MPa) is deviated by 11.19% from standard value. Tensile specimens of HS-G save 60.86% of printing time and 14.72% of cost than HQ-G. This research paper provides a unique way of meeting optimal selection process parameters. Finally, a case study was carried out for the selected application with optimized process parameters.

Keywords Additive manufacturing · PolyJet · Mechanical properties · Printing mode · Surface finish

1 Introduction

Additive manufacturing (AM) technologies is one of the most favourable areas in the manufacturing to produce complex geometrical components [1]. Furthermore, they enable the manufacture of huge variety of prototypes and functional components involving complex geometries [2]. AM needs precise building parameters before design and fabrication [3]. Because of this, it is most essential to reduce manufacturing cost and attain mechanical properties requirements [4]. Unfortunately, factors affecting mechanical property of the 3D printed part and the contributing factors and interactions were not established well [5]. Especially, in PolyJet technology, these factors are not analysed appropriately [6].

In many applications, material properties provided by the manufacturers are not practically suitable, whereas the property of individual material is most important to develop hybrid materials, high strength polymers and biocompatible materials. Therefore, new engineering polymers with diverse characteristics should be developed to expand PolyJet applications. This is certainly to determine life of the 3D printed parts using PolyJet [7]. Further, the need is to examine the effect of process parameters on mechanical properties along with their optimal selection is very important [8]. Understanding the need, this work is focused on investigating the mechanical property of the PolyJet printed parts and further, increasing novel application of PolyJet technology for the development of innovative products [3].

2 Literature review

AM is increasingly adopted for the creation of innovative products and functional parts [9]. The manufacture of functional parts using AM could take advantage of the increased design possibilities to enhance part functionality [10]. This is because traditional or non-traditional machining process such as casting or moulding cannot produce high complex parts without the tooling constraint. If tooling constraints are

✉ Arivazhagan Pugalendhi
arivazhagan.mech02@gmail.com

[1] Department of Mechanical Engineering, Coimbatore Institute of Technology, Civil Aerodrome Post, Coimbatore, TN 641014, India

eliminated, then restrictions were reduced in the field of design for manufacturing and assembly [11]. However, there is a limited comprehensive design for AM [12].

AM techniques provide specific material groups and operate based on unique process mechanism [13]. Currently, there are seven different categories of AM technologies available. Those technologies are operated by different mechanisms. Of the seven mechanisms, four are capable of producing metallic parts and remain capable to produce other materials. There are much advanced technologies like laser powder-bed fusion and selective laser melting available to produce metallic parts [14, 15].

The other AM technology is droplet-based 3D printing; this technology can also produce metallic parts. In this technology, each droplet needs good metallurgical bonding between neighbouring droplets [16, 17]. Compared with selective laser sintering (SLS) and 3D inkjet printers (3DP), the accuracy of the 3D printed healthcare models are high in PolyJet [18]. Study revealed that resins that require lower barrel temperatures and moulding pressures are best suited for making AM tools. Moulding of polypropylene (PP) by using AM tools is found to have a life and is greater than 250 parts [19].

Therefore, it is essential to study the manufacturing and design guidelines for individual processes to achieve optimal mechanical properties [20]. There is a vast assembly of materials with strongly differing properties [21]. The mechanical properties of any material depend on their atomic structure [22]. Therefore, study about the mechanical properties is almost important to study the structure of materials [23]. The atomic structure of the product produced by AM is atomic lattice structure [24].

Even though atomic structure of AM material is unique, but the mechanical properties of it differ [25]. This is certainly because the mechanical properties may change depending on other parameters [26]. In AM, different process parameters like raster angle, orientation, rate of deposition of material, layer thickness and diameter of nozzle remain as some of the process parameters that affect mechanical properties [27].

Strength and accuracy of 3D printed parts are inversely proportional to layer thickness. Orientation of the object towards the building direction gives better result. For example, in case of flat-XY orientation, it provides better tensile properties than upright-ZX and on-edge-XZ orientations [28, 29]. Since during the tensile test, direction of the load is parallel to the filaments of flat specimens, which require the extra load to break the specimen [30]. Further, when it comes to orientation, flat orientation parts have a faster build time than other orientations [31].

The mechanical properties of 3D printed parts with above process parameters affects tensile strength, elongation, shear strength, flexural strength, etc. The researchers and AM machine manufactures test the mechanical properties of their AM material only [32]. Therefore, lots of AM materials are needed to be tested for their mechanical behaviour [33]. For example, in FDM, the optimum layer thickness is 0.5 mm than 0.35 mm and 0.4 mm, optimum infill density is 80% than 40% and 60% and 65° of raster angle is optimum than 45° and 55°. These results reveal that the maximum thickness with higher density of layers gives better mechanical properties [34].

PolyJet AM technology is one such technology that involves in multi-material printing technology available in the market. In addition, this technology can print parts with different textures [35, 36]. This multi-material AM technology can develop different material combinations in different process parameters. This is certainly by more than one base material in different process parameters [37]. This multi-material printing can improve functionality of the printed parts. For example, if rubber layer is inserted in between the rigid layers as like sandwich type, it increases the energy absorbing capability of the AM parts [38].

Zhang et al. [39] proved the improvement of damping properties by staggering geometric patterns of the rigid and elastic materials of Objet Connex 3D printed materials. From this study, equal contribution of the hard and soft phase results are optimal. Another PolyJet study revealed that the optimum parameters are 30 μm layer thickness (high speed), and 90° part orientation with glossy finish and lite support material fill used has better mechanical properties like tensile, shore hardness and surface roughness compared with 16 μm layer thickness (high quality). This is with matte finish, 0° part orientation and heavy support material fill application [40].

In addition, other researchers like Kantareddy et al. [41] utilize the differences in glass transition temperature and elastic moduli of the PolyJet materials to create shape-changing structure also known as 4D printing. Sanders et al. [42] reported the effect of glass transition temperature of VeroBlackPlus, which is higher in larger layer thickness (27 μm) with flat-XY orientation. Hence, the optimum process parameters play a major role in mechanical properties.

Study of dynamic mechanical and thermal analysis of PolyJet printed materials reveal that storage modulus and loss factor of TangoPlus have greater variations compared with VeroWhitePlus, DM 8430 and DM 8420. Complex modulus is not affected by in-plane print direction [43]. In a recent work, Gouzman et al. [44] reported the optimization of the printing and jetting conditions, which permit the production of first bismaleimides (BMI) objects by PolyJet technology, as well as investigate the printed material properties.

This multi-material with different process parameters made AM parts, which has many applications like health care, aerospace and consumer products. Multi-material printing by AM is possible to vary flexibility and hardness of the product [45]. Work carried out in developing customized split insole for diabetic patients using PolyJet technology involved one split insole with various shore hardness [45]. This is impossible to produce by conventional manufacturing system. Therefore, it needs advanced manufacturing technique like AM. The PolyJet AM technology can produce an insole with different

shore hardness. Therefore, mechanical properties like shore hardness play a major role in many health care applications [45]. Therefore, each application needs different texture and mechanical properties [46]. As in previous research, the variable hardness orthotic product is developed with variable shore hardness across the layer of insole [47].

Surface finish is important in many applications. For example, glossy finish is required in automotive industries, many household appliances and health care industry [48]. When it comes to production of glossy finish, its support material is not required to cover entire part, and the glossy finish has better accuracy and higher fatigue life [13, 49]. This research paper studies about the relation between surface finish and layer thickness with respect to mechanical properties of VeroBlue material. So that better combination of multi material printing can be used for many health care applications. The following section explains about material and methods used to study the mechanical properties of fabricated specimens with various process parameters.

3 Materials and methods

The materials and methods used to succeed the objective of this paper are explained in this section. The first subsection deals with machine and material used in this research paper. This is followed by another subsection, which is the most important portion dealing with specimen preparation and process parameters.

3.1 Machine and material

Objet260 Connex, a PolyJet technology from Stratasys, is used for this study. The product manufactured using this machine has the power to simulate a precise look, feel and function of sophisticated finished products. This machine is ideal for various applications, where the product needs to be effectively highlighted with the varying material components in complex or assembled state. It combines an outstanding 16-μm (high quality) and 30-μm (high speed and digital material) high-resolution layer accuracy with a tray size of 255 × 252 × 200 mm [50].

In PolyJet process, droplets of a liquid photopolymer resin is selectively jetted by set of nozzles onto a build tray that is instantly cured by ultraviolet (UV) light. After the solidification of recent layer, the build tray moves downwards in direction (Z axis) by one layer thickness. This continuous deposition and curing process is repeated until the last layer of the object. Assembly of jetting head moves in X and Y axis which consists of 4 printing heads for model materials, 4 printing heads for support materials, UV lamps and levelling roller [42, 51]. Figure 1 represents the schematic illustration of the PolyJet 3D printing mechanism.

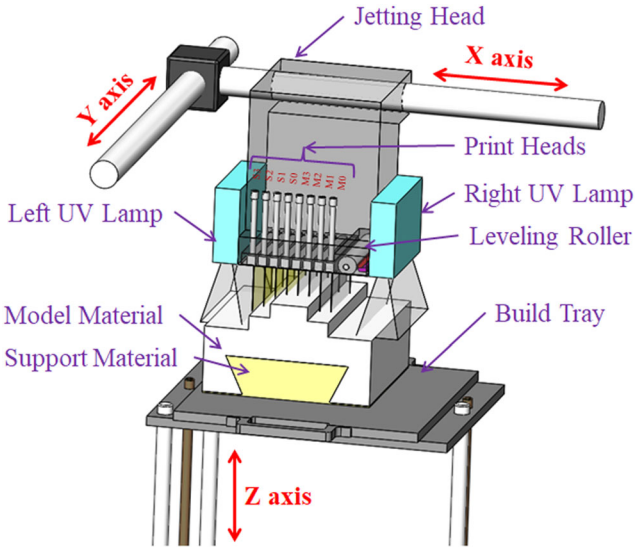

Fig. 1 A schematic illustration of the PolyJet 3D printing mechanism

This machine also has the most extensive range of materials with different material properties; it prints any product with 15 material properties simultaneously on a single part. Here, VeroBlue material is chosen to study the effects of mechanical properties. It is certainly because VeroBlue involves minimum material cost compared with mostly used PolyJet materials of VeroClear, TangoPlus and VeroWhite, and its percentage of deviation in material cost is 22.86%, 22.78% and 2.79%, respectively. VeroBlue is a rigid opaque collection of material, which provides the best detail of visualization, without glare or darkness. The mechanical property of VeroBlue is shown in Table 1. FullCure 705 non-toxic gel-like photopolymer is used as a support material.

The fabricated product is then tested by considering standard testing specimens for tensile (American Society for Testing and Materials (ASTM) D638) and flexural (ASTM D790) with 3.2 mm thickness for both specimens and shore hardness (ASTM D2240) [52–54]. The tensile and flexural tests were performed by zwick universal testing machine having the capacity ranges of 0–100KN, speed of 50 mm/min and constant environment of 72 °F. Shore hardness is tested by using a Shore D durometer having the capacity ranges of 0–100 HD and accuracy of 0.5 HD in 68–70 °F temperature.

Modelling of specimens and the file conversion of part file into STL file is done by SolidWorks 2016. Machine interfacing software of Objet Studio is used for pre-processing such as part orientation, selection of material, printing mode and finish type.

3.2 Specimen preparation and process parameters

In this study, three mechanical properties were tested and compared. Standard sized specimens for the tensile, flexural and shore hardness tests were performed according to specific

Table 1 Mechanical properties of VeroBlue (source: Stratasys)

Mechanical properties	Test method	Value (metric unit)
Colour/appearance	Visual	Pale blue
Tensile strength	ASTM D638	50–60 MPa
Elongation at break	ASTM D638	15–25%
Modulus of elasticity	ASTM D638	2000–3000 MPa
Flexural strength	ASTM D790	60–70 MPa
Flexural modulus	ASTM D790	1900–2500 MPa
Izod notched impact	ASTM D256	20–30 J/m
Shore D hardness	–	83–86 D
Heat deflection temperature	ASTM D648 @ 1.82 MPa	45–50 °C

standards. Tensile test standards are ISO 527 and ASTM D638. These two methods are technically equal but do not provide comparable results because of the test speeds, specimen sizes, method of result and as the determination differ in some respects. So, mostly ASTM D638 is used in determining test results. In this study, due to minimum material consumption and printing cost, the type I tensile specimen is selected. Dimensions of the dog-bone shaped tensile specimen are 165 × 19 × 3.2 mm with 50 mm gauge.

The flexural test is used to measure the force required to bend the beam under three-point loading conditions [55], while flexural modulus is carried out for indication of material's stiffness when flexed [56]. ASTM D790 is the method for determining the flexural properties (bending properties) of reinforced and unreinforced plastics and electrical insulation materials. Dimensions of the flexural specimen are 127 × 12.7 × 3.2 mm having rectangular cross-section.

Shore hardness of rigid and harder plastic materials is measured by scale D. According to ASTM D2240, dimensions of shore hardness specimen are circular disc of Ø25 × 10 mm. After the design of selected specimens, pre-processing is performed by Objet Studio for interaction of the PolyJet machine. In this study, specimens are printed by high quality (HQ) and high speed (HS) printing modes with two different finish types, namely matte and glossy. Layer thickness of HQ is 16 μ and of HS is 30 μ. In matte finish (M), required part is fully covered by support material. Glossy finish (G) reflects the light and beautiful in aesthetics. The specimens are categorized into four different types as: HQ-M, HS-M, HQ-G and HS-G, respectively. As per the many related research, all the specimens are oriented in lengthwise direction. Figure 2 illustrates the orientation of all test specimens arranged in build tray of Objet Studio window. For tensile and flexural test, three specimens per print and for

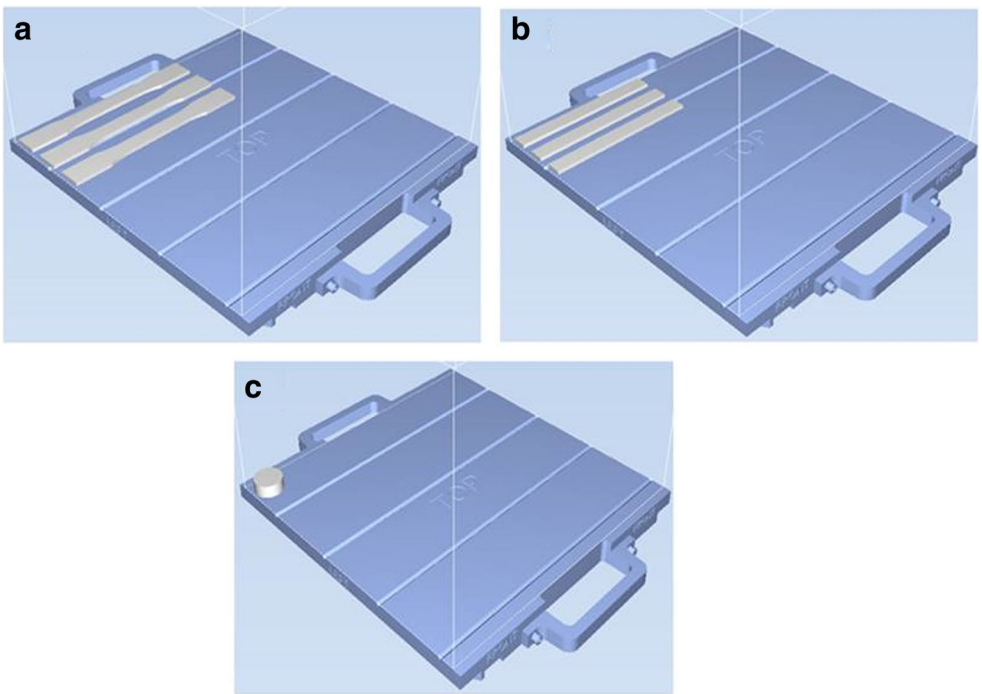

Fig. 2 Orientation of test specimens on Objet Studio

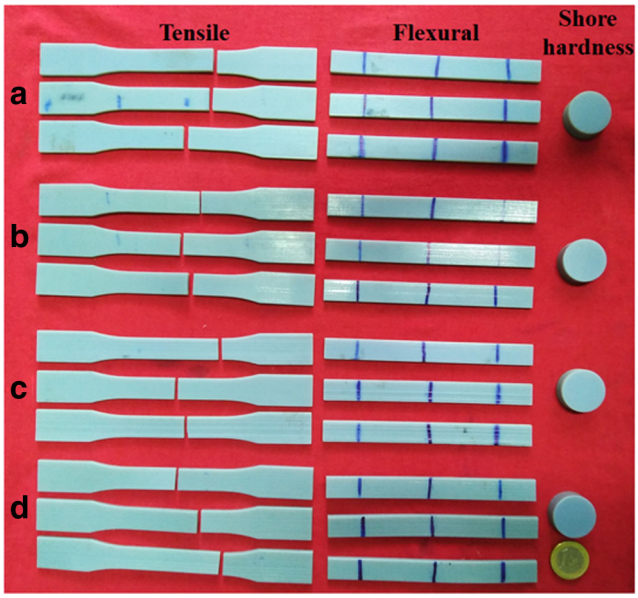

Fig. 3 Tensile, flexural and shore hardness tested specimens

shore hardness, one specimen is taken for testing, which are shown in Fig. 2a, b, c, respectively.

4 Results and discussion

This section discusses about the mechanical properties: tensile strength, elongation at break, flexural strength, flexural modulus and shore hardness. Material consumption of both model and support material with required printing time of all types and its printing cost are also discussed. The printed specimens are immediately sent for the testing after completion of post-processing, and it does not exceed the more than a day. Figure 3 illustrates the tested specimens for tensile strength, flexural strength and shore hardness. Figure 3A represents the HQ-M test specimens of tensile test, flexural test and shore hardness test from left to right. Similarly, Fig. 3B, C and D represents the HQ-G, HS-M and HS-G, respectively.

4.1 Tensile test

Printing details of tensile test specimens are tabulated in Table 2, this further includes model material consumption, support material consumption, printing time and cost. It could be seen from Table 2 that all the factors are high in matte finish compared with glossy finish. This is certainly because, in matte finish, the fabricated parts are fully immersed in support material, but it gives a uniform finish throughout the component. HQ-M requires more materials, higher printing time, and these are expensive to print the specimens than any other type of printing. However, HS-G is vice-versa of all the above mentioned parameters. This is because comparing between both glossy finishes (HQ-G and HS-G) reveals the percentage of differences in model material and support material, which is 6.97 and 7.69%. Similarly, HS-G saves about 60.86% of printing time and 14.72% of cost with respect to HQ-G.

The tensile strength results shown in Fig. 4 have two different vertical axes like primary and secondary. The primary axis denotes tensile strength in MPa, and the secondary axis denotes average tensile strength for each of the fabricated method. In addition, the horizontal axis denotes specimen numbers of HQ-M, HQ-G, HS-M and HS-G. Finally, the bar chart shows tensile strength of each sample specimen.

Figure 4 shows the tensile test results of all tensile test specimens. There are three tensile specimens that were produced in a single print. Figure 4 clarifies that average tensile strength of the HS-G specimen has peak value of 49.47 MPa, and HQ-M has lowest average tensile strength value of 47.4 MPa. Results of all the average tensile strength values are lesser than boundary of the standard value (50–60 MPa). By comparing the HS-G and HQ-G, the average tensile strength is 1.31% higher in HS-G. Additionally, in an average tensile strength values of HS-G, it is deviated by 11.18% from standard average tensile strength value as shown in Table 1.

Table 2 Specimen preparation for tensile test

S.No	Name		Tensile specimens (3 pieces)			
			Model material consumption (gram)	Support material consumption (gram)	Printing time (minutes)	Cost (USD)
1	High quality–matte	HQ-M	48	27	39	37.12
2	High quality–glossy	HQ-G	46	14	37	32.88
3	High speed–matte	HS-M	44	25	24	32.03
4	High speed–glossy	HS-G	43	13	23	28.66

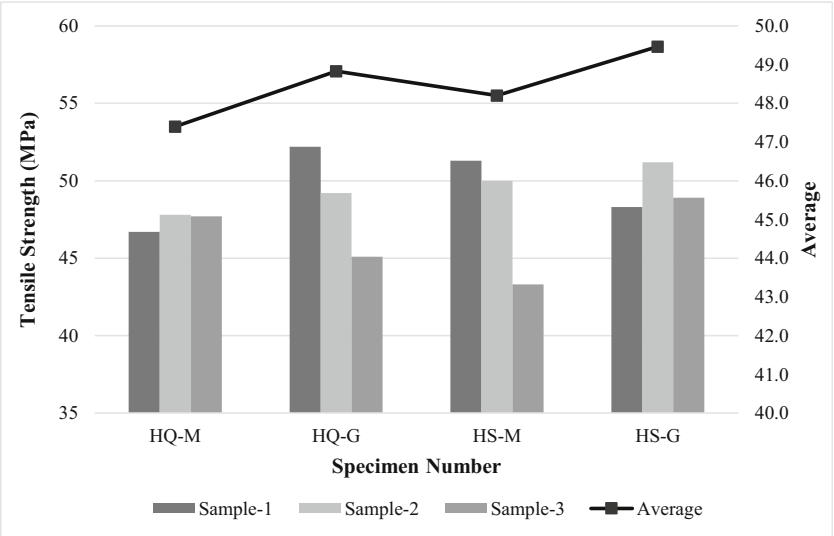

Fig. 4 Tensile strength

Figure 5 illustrates the differences in elongation at break. These results are obtained from the tensile test. HS-G has the maximum average elongation at break of 34.33%, and the minimum value of HQ-M is 26.66%. All the values exceeds the upper boundary of the standard value (15–25%). Percentage of deviation in average elongation at break is 10.75% compared with HS-G and HQ-G. Additionally, in an average elongation at break values of HS-G, it is deviated by 71.66% from the standard value (20%) as shown in Table 1.

4.2 Flexural test

The preparation of flexural test specimens is tabulated in Table 3. Here, the model material consumption gradually decreases by 1 g from HQ-M to HS-G. Similar to tensile test, material consumption, required printing time of the specimen and cost are higher in HQ-M and lower in HS-G. Noticeably, glossy finish is less expensive and consumes lesser time to print compared with matte finish. Cost of HS-G is 34.29% cheaper than HQ-M

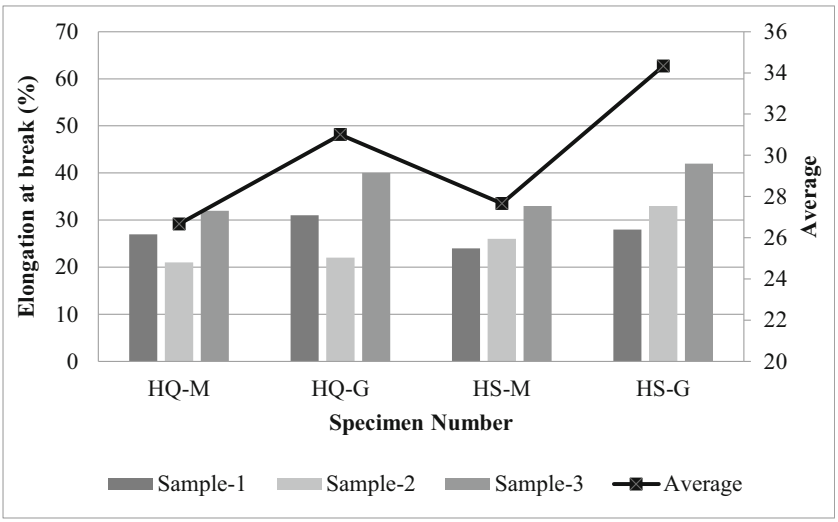

Fig. 5 Elongation at break

Table 3 Specimen preparation for flexural test

S.No	Name		Flexural specimens (3 pieces)			
			Model material consumption (gram)	Support material consumption (gram)	Printing time (minutes)	Cost (USD)
1	High quality–matte	HQ-M	30	19	33	26.12
2	High quality–glossy	HQ-G	29	10	28	22.66
3	High speed–matte	HS-M	28	17	20	22.30
4	High speed–glossy	HS-G	27	9	17	19.45

and 16.50% cheaper than HQ-G. Similarly, HS-G printing time is less by 94.11% and 64.70% compared with HQ-M and HQ-G, respectively.

Figure 6 infers that there is a variation in the flexural strength value. From this result, HS-G, HQ-G, HS-M and HQ-M obtained the highest from lowest values, respectively. Compared with HS-G (25.83 MPa) and HQ-M, the flexural strength deviates by 27.67%. Flexural strength of HQ-G is 7.49% lower than HS-G. Results of all the average flexural strength values are very minimum as compared with the standard lower boundary value (60–70 MPa). Highest value of HS-G is 151.63%, which deviates from standard value.

Differences in flexural modulus of all modes are displayed in Fig. 7. It is understood that HS-G value of 1009.66 MPa is higher compared with all other combinations, and HS-M gives the lowest value of 756.33 MPa. Similar to flexural strength, all the values of flexural modulus is also very minimum than standard lower boundary values (1900–2500 MPa). Thereby, it could be seen that the HS-G value is 1.54% higher than HQ-G and 117.89% lower than standard value.

4.3 Shore hardness test

Printing details of shore hardness test specimens are tabulated in Table 4. Model material consumption is same for HQ-M and HQ-S as well as HS-M and HS-G. Similarly, printing time of HQ-M and HQ-G is same as HS-M, and HS-G is more or less the same. Nevertheless, support material consumption is same for HQ-M and HS-M as well as HQ-G and HS-G. Therefore, HQ-G model material consumption is 10% higher than HS-G, and there is no change in support material consumption. Similarly, HS-G printing time and cost is lesser than HQ-G with 66.66 and 27.50%, respectively. Specimen preparation for the entire test reveals that the percentage of difference is directly proportional to the size of the components to be printed.

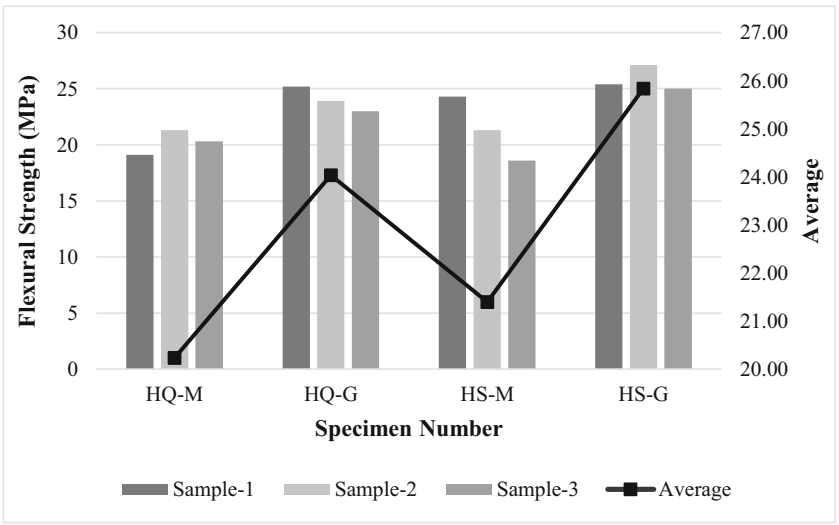

Fig. 6 Flexural strength

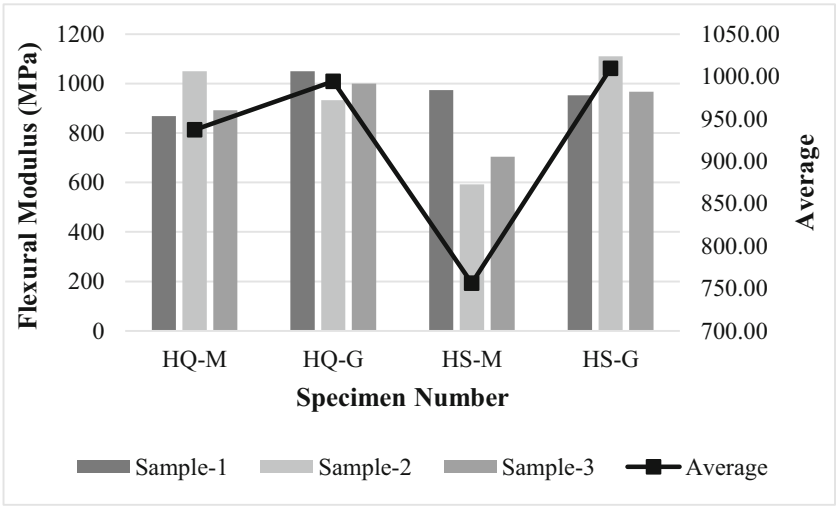

Fig. 7 Flexural modulus

Table 4 Specimen preparation for shore hardness

S.No	Name		Single hardness specimen			
			Model material consumption (gram)	Support material consumption (gram)	Printing time (minutes)	Cost (USD)
1	High quality–matte	HQ-M	11	5	36	15.01
2	High quality–glossy	HQ-G	11	3	35	14.37
3	High speed–matte	HS-M	10	5	22	11.90
4	High speed–glossy	HS-G	10	3	21	11.27

Figure 8 also has two axes similar to the other and has six trails; therefore, there are six bars as shown in graph. Figure 8 reveals six trails/indention on single shore hardness specimen, and it elucidates that the HS-G has highest average shore hardness 80.16 D. Then, HS-M has lowest average shore hardness of 75.91 D. Overall, HS-G shore hardness value is 0.84% higher than HQ-G and 5.40% lower than standard average shore hardness (84.5 D). Standard lower boundary value of shore hardness (83–86 D) is higher than values of all types.

From the above, it could be concluded that the product fabricated using high speed with glossy finish will have high strength in terms of tensile, flexural and shore hardness tests. Except elongation at break, all the test results are lesser than

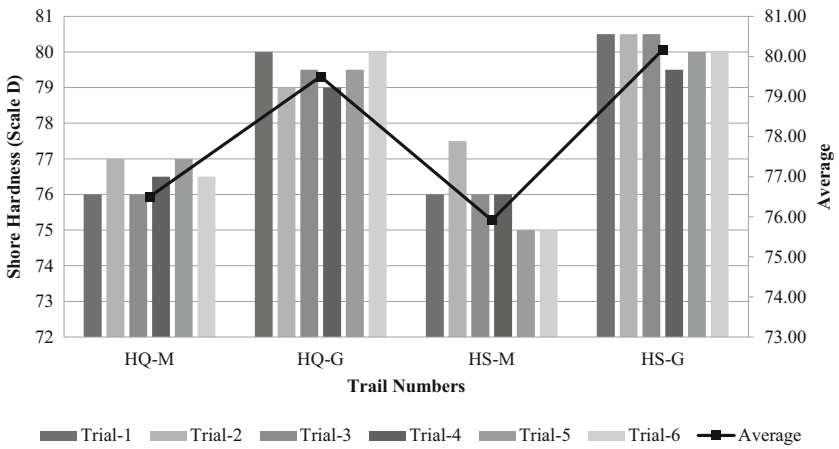

Fig. 8 Shore hardness

lower boundary of the standard values. This is because the time gap between each layer in high-speed process is less. High-speed process mode has larger layer thickness as well as lowest printing time. Here, each layer during high-speed process mode may bind perfectly than high quality mode.

In addition, due to the non-contact between the support materials with the build part, the glossy surface finish has less peaks and valleys in its surface. Finally, after the post-processing, wherever support material is in connection with final part, it creates minute sharp edges. Generally, sharp edges initiate the crack propagations. These are all the major reason to increase the test results in HS-G mode. Faster printing time and minimum support material consumption of HS-G results in cheaper printing cost than other types.

In this research, matte finished parts exhibit lower mechanical strength and glossy finished parts unveil higher strength as stated by Moore and Williams [49] and Yap et al. [13]. With higher thickness of an individual layer (HS 30 μ), will also have the higher mechanical properties compared with HQ mode (16 μ). Conferring to the study of Sufiiarov et al. [29] and Kreisköther et al. [40], the above result conflicts with this research paper. Nevertheless, according to study, 0.1125 mm layer thickness is better than 0.0875, 0.1 and 0.125 mm layer thickness [28], because minimum layer thickness does not give better strength in all the cases.

5 Case study

As per the test results and preparation of specimens, one functional prototype and one concept prototype were printed by HS-G combination. Propeller for drone and human ear is referred as a functional prototype and concept prototype, respectively. Finished product of propeller and human ear are shown in Fig. 9a and b, respectively. Propeller is directly assembled with the drone and perfectly fitted with the motor shaft. Main function of the propeller is used to create the thrust force and actuate the drone as per the joystick actuation. It can withstand the wind force and its tightening force of screw. Therefore, force calculations and main design aspects are clearly analysed before printing the prototype.

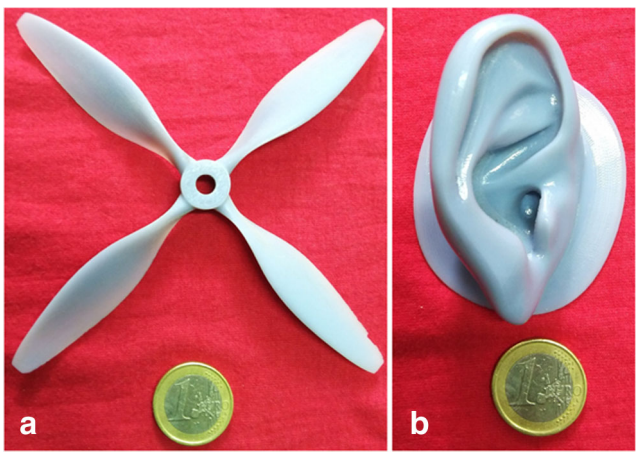

Fig. 9 PolyJet printed parts. **a** Propeller. **b** Human ear

Another prototype of human ear is printed and act as concept prototype. It is used for wider application like sample for doctors to practise and patients' understanding, fixture for customized hearing machine, it is easy to use and it decorates the doctors table along with the study material for skin grafting. Ear prototype is printed from the scan data and smoothening is done by geomagic freeform plus. Maximum dimensions of the drone propeller and human ear is Ø145.25 × 11.72 mm and 52.9 × 64.77 × 34.4 mm, respectively. From these case studies, it could be infered that VeroBlue material is best suitable for all types of prototypes with less cost without sacrificing quality of the prototype.

6 Conclusion

The objective of this paper is to identify the best combination for VeroBlue material in Objet260 Connex from four type of combinations. Printing mode and finish type is segregated based on the combinations. Therefore, this paper identifies that HS-G as a suitable combination for VeroBlue in PolyJet process. This is because this high-speed printing mode prints faster, is cheaper and involves lesser material consumption. PolyJet printed tensile specimens in HS-G saves about 60.86% printing time and 14.72% cost than HQ-G. In flexural specimens, printing time and cost of the HS-G is 64.70% and 16.50% lesser than HQ-G. Correspondingly, printing time and cost of HS-G is 66.66% and 27.50% lesser than HQ-G, respectively.

In addition, the glossy finish has less peaks and valleys; therefore, this HS-G has highest values in all results. Finally, this paper concludes that the high-speed printing mode with glossy surface finish is suitable for VeroBlue in PolyJet technology. Tensile strength and elongation at break of HS-G is 49.47 MPa and 34.33%, respectively. HS-G specimens have the flexural strength of 25.83 MPa and flexural modulus of 1009.67 MPa. Similarly, shore hardness of HS-G is 80.16 D. Through this work, it was realized that VeroBlue can also be used to produce many human organs for training surgeons to practise; it is under the circumstance of where colour is not important. This optimal selection is also used in development of hybrid materials and digital materials to increase the PolyJet applications.

7 Future work

Further, this study extends to other available material in PolyJet machine, which includes the temperature difference in pre-processing and post-processing and time gap between printing and testing. Other mechanical tests of surface roughness, fatigue strength and compressive strength etc. can also be evaluated.

Funding information We gratefully acknowledge the financial support for establishing the Centre of Excellence in Manufacturing Sciences (CoEMS) at Coimbatore Institute of Technology, Coimbatore; India from Ministry of Human-Resource Development (MHRD), Govt of India where the sample/R&D work is carried out.

References

1. Khajavi SH, Partanen J, Holmström J (2014) Additive manufacturing in the spare parts supply chain. Comput Ind 65(1):50–63. https://doi.org/10.1016/j.compind.2013.07.008
2. Petrovic V, Vicente Haro Gonzalez J, Jordá Ferrando O, Delgado Gordillo J, Ramón Blasco Puchades J, Portolés Griñan L (2011) Additive layered manufacturing: sectors of industrial application shown through case studies. Int J Prod Res 49(4):1061–1079. https://doi.org/10.1080/00207540903479786
3. Gao W, Zhang Y, Ramanujan D, Ramani K, Chen Y, Williams CB, Wang CCL, Shin YC, Zhang S, Zavattieri PD (2015) The status, challenges, and future of additive manufacturing in engineering. Comput Aided Des 69:65–89. https://doi.org/10.1016/j.cad.2015.04.001
4. Atzeni E, Salmi A (2012) Economics of additive manufacturing for end-usable metal parts. Int J Adv Manuf Technol 62(9):1147–1155. https://doi.org/10.1007/s00170-011-3878-1
5. Lanzotti A, Grasso M, Staiano G, Martorelli M (2015) The impact of process parameters on mechanical properties of parts fabricated in PLA with an open-source 3-D printer. Rapid Prototyp J 21(5):604–617. https://doi.org/10.1108/RPJ-09-2014-0135
6. Barclift MW, Williams C (2012) Examining variability in the mechanical properties of parts manufactured via polyjet direct 3D printing. In: International. Solid Freeform Fabrication Symposium Proceddings, Austin
7. Gaynor AT, Meisel NA, Williams CB, Guest JK (2014) Multiple-material topology optimization of compliant mechanisms created via PolyJet three-dimensional printing. J Manuf Sci Eng 136(6). https://doi.org/10.1115/1.4028439
8. Lee BH, Abdullah J, Khan ZA (2005) Optimization of rapid prototyping parameters for production of flexible ABS object. J Mater Process Technol 169(1):54–61. https://doi.org/10.1016/j.jmatprotec.2005.02.259
9. Conner BP, Manogharan GP, Martof AN, Rodomsky LM, Rodomsky CM, Jordan DC, Limperos JW (2014) Making sense of 3-D printing: creating a map of additive manufacturing products and services. Addit Manuf 1-4:64–76. https://doi.org/10.1016/j.addma.2014.08.005
10. Tang Y, Yang S, Zhao YF (2016) Sustainable design for additive manufacturing through functionality integration and part consolidation. In: Muthu SS, Savalani MM (eds) Handbook of sustainability in additive manufacturing, vol 1. Springer, Singapore, pp 101–144. https://doi.org/10.1007/978-981-10-0549-7_6
11. Rosato DV, Rosato DV, Rosato MV (2004) 11 - casting. In: Rosato DV, Rosato DV, Rosato MV (eds) Plastic product material and process selection handbook. Elsevier, Oxford, pp 394–405. https://doi.org/10.1016/B978-185617431-2/50014-1
12. Shamsaei N, Yadollahi A, Bian L, Thompson SM (2015) An overview of direct laser deposition for additive manufacturing; part II: mechanical behavior, process parameter optimization and control. Addit Manuf 8:12–35. https://doi.org/10.1016/j.addma.2015.07.002
13. Yap YL, Wang C, Sing SL, Dikshit V, Yeong WY, Wei J (2017) Material jetting additive manufacturing: an experimental study using designed metrological benchmarks. Precis Eng 50:275–285. https://doi.org/10.1016/j.precisioneng.2017.05.015
14. Tapia G, Khairallah S, Matthews M, King WE, Elwany A (2018) Gaussian process-based surrogate modeling framework for process planning in laser powder-bed fusion additive manufacturing of 316L stainless steel. Int J Adv Manuf Technol 94(9):3591–3603. https://doi.org/10.1007/s00170-017-1045-z
15. Sing SL, Wiria FE, Yeong WY (2018) Selective laser melting of lattice structures: a statistical approach to manufacturability and mechanical behavior. Robot Comput Integr Manuf 49:170–180. https://doi.org/10.1016/j.rcim.2017.06.006
16. Yi H, Qi L, Luo J, Zhang D, Li H, Hou X (2018) Effect of the surface morphology of solidified droplet on remelting between neighboring aluminum droplets. Int J Mach Tools Manuf 130-131:1–11. https://doi.org/10.1016/j.ijmachtools.2018.03.006
17. Yi H, Qi L, Luo J, Li N (2019) Hole-defects in soluble core assisted aluminum droplet printing: metallurgical mechanisms and elimination methods. Appl Therm Eng 148:1183–1193. https://doi.org/10.1016/j.applthermaleng.2018.12.013
18. Ramola M (2019) On the adoption of additive manufacturing in healthcare: a literature review. J Manuf Technol Manag 30(1):48–69. https://doi.org/10.1108/JMTM-03-2018-0094
19. Nelson JW, LaValle JJ, Kautzman BD, Dworshak J, Johnson EM, Ulven C (2017) Injection molding with an additive manufacturing tool study shows that 3D printed tools can create parts comparable to those made with P20 tools, at a much lower cost and lead time. Plast Eng 73:60–66
20. Ashby MF, Bréchet YJM, Cebon D, Salvo L (2004) Selection strategies for materials and processes. Mater Des 25(1):51–67. https://doi.org/10.1016/S0261-3069(03)00159-6
21. Andres RP, Averback RS, Brown WL, Brus LE, Goddard WA, Kaldor A, Louie SG, Moscovits M, Peercy PS, Riley SJ, Siegel RW, Spaepen F, Wang Y (2011) Research opportunities on clusters and cluster-assembled materials—a Department of Energy, Council on Materials Science Panel Report. J Mater Res 4(3):704–736. https://doi.org/10.1557/JMR.1989.0704
22. Salvetat JP, Bonard JM, Thomson NH, Kulik AJ, Forró L, Benoit W, Zuppiroli L (1999) Mechanical properties of carbon nanotubes. Appl Phys A 69(3):255–260. https://doi.org/10.1007/s003390050999
23. Sahoo S (2017) Simulation study on rapid solidification of eutectic Al-Cu alloy: a molecular dynamics approach. Int J Comput Mater Sci Surf Eng 7(1):18–25
24. Martukanitz R, Michaleris P, Palmer T, DebRoy T, Liu Z-K, Otis R, Heo TW, Chen L-Q (2014) Toward an integrated computational system for describing the additive manufacturing process for metallic materials. Addit Manuf 1-4:52–63. https://doi.org/10.1016/j.addma.2014.09.002
25. Gu DD, Meiners W, Wissenbach K, Poprawe R (2012) Laser additive manufacturing of metallic components: materials, processes and mechanisms. Int Mater Rev 57(3):133–164. https://doi.org/10.1179/1743280411Y.0000000014
26. Khorasani AM, Yazdi MRS, Safizadeh MS (2012) Analysis of machining parameters effects on surface roughness: a review. Int J Comput Mater Sci Surf Eng 5(1):68–84. https://doi.org/10.1504/ijcmsse.2012.049055

27. Ahn SH, Montero M, Odell D, Roundy S, Wright PK (2002) Anisotropic material properties of fused deposition modeling ABS. Rapid Prototyp J 8(4):248–257. https://doi.org/10.1108/13552540210441166
28. Farzadi A, Solati-Hashjin M, Asadi-Eydivand M, Abu Osman NA (2014) Effect of layer thickness and printing orientation on mechanical properties and dimensional accuracy of 3D printed porous samples for bone tissue engineering. PLoS One 9(9):e108252. https://doi.org/10.1371/journal.pone.0108252
29. Sufiiarov VS, Popovich AA, Borisov EV, Polozov IA, Masaylo DV, Orlov AV (2017) The effect of layer thickness at selective laser melting. Procedia Eng 174:126–134. https://doi.org/10.1016/j.proeng.2017.01.179
30. Vukasovic T, Vivanco JF, Celentano D, García-Herrera C (2019) Characterization of the mechanical response of thermoplastic parts fabricated with 3D printing. Int J Adv Manuf Technol 104:4207–4218. https://doi.org/10.1007/s00170-019-04194-z
31. Bikas H, Lianos AK, Stavropoulos P (2019) A design framework for additive manufacturing. Int J Adv Manuf Technol 103(9):3769–3783. https://doi.org/10.1007/s00170-019-03627-z
32. Tofail SAM, Koumoulos EP, Bandyopadhyay A, Bose S, O'Donoghue L, Charitidis C (2018) Additive manufacturing: scientific and technological challenges, market uptake and opportunities. Mater Today 21(1):22–37. https://doi.org/10.1016/j.mattod.2017.07.001
33. Park S-I, Rosen DW, S-k C, Duty CE (2014) Effective mechanical properties of lattice material fabricated by material extrusion additive manufacturing. Addit Manuf 1-4:12–23. https://doi.org/10.1016/j.addma.2014.07.002
34. Samykano M, Selvamani SK, Kadirgama K, Ngui WK, Kanagaraj G, Sudhakar K (2019) Mechanical property of FDM printed ABS: influence of printing parameters. Int J Adv Manuf Technol 102(9):2779–2796. https://doi.org/10.1007/s00170-019-03313-0
35. Thompson MK, Moroni G, Vaneker T, Fadel G, Campbell RI, Gibson I, Bernard A, Schulz J, Graf P, Ahuja B, Martina F (2016) Design for additive manufacturing: trends, opportunities, considerations, and constraints. CIRP Ann 65(2):737–760. https://doi.org/10.1016/j.cirp.2016.05.004
36. Ngo TD, Kashani A, Imbalzano G, Nguyen KTQ, Hui D (2018) Additive manufacturing (3D printing): a review of materials, methods, applications and challenges. Compos Part B 143:172–196. https://doi.org/10.1016/j.compositesb.2018.02.012
37. Choi J-W, Kim H-C, Wicker R (2011) Multi-material stereolithography. J Mater Process Technol 211(3):318–328. https://doi.org/10.1016/j.jmatprotec.2010.10.003
38. Rajendra Boopathy V (2019) Energy absorbing capability of additive manufactured multi-material honeycomb structure. Rapid Prototyp J 25(3):623–629. https://doi.org/10.1108/RPJ-03-2018-0066
39. Zhang P, Heyne MA, To AC (2015) Biomimetic staggered composites with highly enhanced energy dissipation: modeling, 3D printing, and testing. J Mech Phys Solids 83:285–300. https://doi.org/10.1016/j.jmps.2015.06.015
40. Kreisköther K, Kampker A, Reinders C (2017) Material and parameter analysis of the polyjet process for mold making using design of experiments. World J Nucl Sci Technol:219–226
41. Kantareddy SNR, Simpson TW, Ounaies Z, Frecker M (2016) 3d printing of shape changing polymer structures: design and characterization of materials. In: Bourell DL, Crawford RH, Seepersad CC, Beaman JJ, Fish S, Marcus H (eds) Proceedings of the 26th Annual International Solid Freeform Fabrication Symposium – An Additive Manufacturing Conference, Texas. Verlag nicht ermittelbar,
42. Sanders J, Wei X, Pei Z (2019) Experimental investigation of Stratasys J750 PolyJet printer: effects of orientation and layer thickness on thermal glass transition temperature
43. Reichl KK, Inman DJ (2018) Dynamic mechanical and thermal analyses of Objet Connex 3D printed materials. Exp Tech 42(1):19–25. https://doi.org/10.1007/s40799-017-0223-0
44. Gouzman I, Atar N, Grossman E, Verker R, Bolker A, Pokrass M, Sultan S, Sinwani O, Wagner A, Lück T, Seifarth C (2019) 3D printing of bismaleimides: from new ink formulation to printed thermosetting polymer objects. Adv Mater Technol 0(0):1–8. https://doi.org/10.1002/admt.201900368
45. Ganesan S, Ranganathan R (2018) Design and development of customised split insole using additive manufacturing technique. Int J Rapid Manuf 7(4):295–309. https://doi.org/10.1504/ijrapidm.2018.095783
46. Agnew SR, Yoo MH, Tomé CN (2001) Application of texture simulation to understanding mechanical behavior of Mg and solid solution alloys containing Li or Y. Acta Mater 49(20):4277–4289. https://doi.org/10.1016/S1359-6454(01)00297-X
47. Desjardins J, Stanley SE, Przestrzelski B, Pruett TC, Hoeffner SL, Kaluf BD (2016) Variable hardness orthotic. Google patents
48. Biris AS, Mazumder MK, Yurteri CU, Sims RA, Snodgrass J, De S (2001) Gloss and texture control of powder coated films. Part Sci Technol 19(3):199–217. https://doi.org/10.1080/02726350290057804
49. Moore JP, Williams CB (2015) Fatigue properties of parts printed by PolyJet material jetting. Rapid Prototyp J 21(6):675–685. https://doi.org/10.1108/RPJ-03-2014-0031
50. Stratasys (2016) Objet260 Connex3
51. Zorzetto L, Ruffoni D (2019) Wood-inspired 3D-printed helical composites with tunable and enhanced mechanical performance. Adv Funct Mater 29(1):1805888. https://doi.org/10.1002/adfm.201805888
52. D638–14 A (2014) Standard test method for tensile properties of plastics. ASTM International, West Conshohocken
53. D790-15e2 A (2015) Standard test methods for flexural properties of unreinforced and reinforced plastics and electrical insulating materials. ASTM International, West Conshohocken
54. D2240–15 A (2015) Standard test method for rubber property—durometer hardness. ASTM International, West Conshohocken
55. Lenard JG (2014) 13 - Severe Plastic Deformation – Accumulative Roll Bonding11Most of the information in this chapter was provided by Dr. Krallics of the Budapest University of Technology and Economics. The experimental portion is based on Krallics and Lenard. In: Lenard JG (ed) Primer on flat rolling, 2nd edn. Elsevier, Oxford, pp 303–322. https://doi.org/10.1016/B978-0-08-099418-5.00013-5
56. Shrivastava A (2018) 3 - plastic properties and testing. In: Shrivastava A (ed) Introduction to plastics engineering. William Andrew publishing, pp 49–110. https://doi.org/10.1016/B978-0-323-39500-7.00003-4